A Quasi-Dynamic Energy Function Method for Out-of-Step Prediction under Line Outages

Xiaowen Su, Zhenping Guo, Kai Sun, *Senior Member, IEEE*

***Abstract*—This paper proposes an energy function method that can evaluate power system dynamic behaviors, especially on whether synchronization can be achieved or not after line outages by quasi-dynamic simulation instead of time consuming dynamic simulations. To judge the synchronization of generation, potential energy and energy dissipation of the system are considered in the proposed energy function. By using the energy function, whether the equilibrium before line outages stays inside the basin of attraction of the equilibrium after line outages can be predicted. The proposed method is tested on the IEEE 39-bus system by dynamic simulations. It is shown that the proposed method can correctly predict the synchronization condition of generators.**

***Index Terms*—energy function, synchronization condition, prediction, line outages**

I. Introduction

Power system transient stability are typically evaluated by three approaches. One approach is the time domain dynamic simulation of the system. The dynamic simulation can provide relatively accurate evaluation of the system transient behaviors according to the transient stability criterion, but the time domain simulation can be time consuming or computational inefficient when a large power system needs to be simulated for an extended time period, e.g. in a scenario of cascading outages. And the dynamic simulation can hardly provide any analytical insights of the system transient stability based on system parameters. Another approach is to utilize machine learning algorithms, which are data-driven methods to evaluate the system stability [1-4]. This approach can predict the system transient stability behaviors when the system response measurement data are available, but this approach heavily relies on the quality and the quantify of the data. The third approach is the direct method, which is to evaluate the transient energy of the system and comparing the transient energy with a threshold to predict on whether the system is transiently stable or not [5-10]. The direct method is also known as the energy function method. The energy of the system can be calculated via the system parameters and state variables. Although the energy function method may subject to an accuracy issue since general energy functions do not exist for multi-machine power systems with large losses, the energy function method can still be applicable to the system with small losses [11]. The energy function can be regarded as a local Lyapunov function [12], so the energy function method still provides a considerable results to evaluate system transient stability due to its fast evaluation speed and its capability of providing the analytical insights.

In power system planning and operations, quasi-dynamic simulations or steady-state simulations are often used. They can be applied to evaluate the system equilibrium. The equilibrium before line outages and the equilibrium after line outages can be evaluated by power flow solutions in quasi-dynamic simulations, such as optimal power flow. However, quasi-dynamic simulation is not necessary to provide whether the equilibrium before line outages can safely transition to a new equilibrium after the line outages without violating the transient stability criterion, such as generation synchronization. So this paper is mainly focused on fast evaluation of the generation synchronization subjected to line outages based on the proposed energy function method. Quasi-dynamic simulations in this paper consider a disturbance that causes one, two or three line outages. There are some potential applications of the proposed prediction method, e.g., 1). for enhancing quasi-dynamic simulation of cascading outages by OPA methods [19-21]; 2). for early warning of angular instability and conducting controlled system separation/islanding [14-18].

The rest of this paper is organized as follows. Section II proposes an energy function method and describes its principle, and Section III implements a case study on the IEEE 39-bus system. The energy function method is applied to the system for evaluating system transient stability subjected to $N-1$, $N-2$ and $N-3$ line outages.

II. Energy Function Method

In quasi-dynamic power system simulation, power flows are solved. If line outages happened, one can re-evaluate new power flows with updated network information and topology. Without a dynamic simulation, it is hardly to know whether the equilibrium before line outages can safely transition to a new equilibrium after the line outages without violating the transient stability criterion. However, dynamic simulation can be time consuming, so this paper applies an energy function method to evaluate whether the equilibrium before the disturbance of line outages is in the basin of attraction of the equilibrium after line outages. In a dynamic system, equilibrium is a vector that consists of rotor angles and speeds, while the equilibrium estimated from the power flow solutions of the system can only provide information about rotor angles, then how the energy function can be applied in absence of speeds? Since there is no rotor speed difference between the pre-disturbance system and the post-disturbance system,

This work was supported in part by NSF grants ECCS-1553863 and in part by the ERC Program of the NSF and DOE under grant EEC-1041877. X. Su, Z. Guo and K. Sun are with the Department of Electrical Engineering and Computer science, University of Tennessee, Knoxvill, USA. (emails:xsu2@vols.utk.edu, zguo19@vols.utk.edu, kaisun@utk.edu)

2022 IEEE Power & Energy Society General Meeting (PESGM) | 978-1-6654-0823-3/22/$31.00 ©2022 IEEE | DOI: 10.1109/PESGM48719.2022.9916948

978-1-6654-0823-3/22/$31.00 ©2022 IEEE

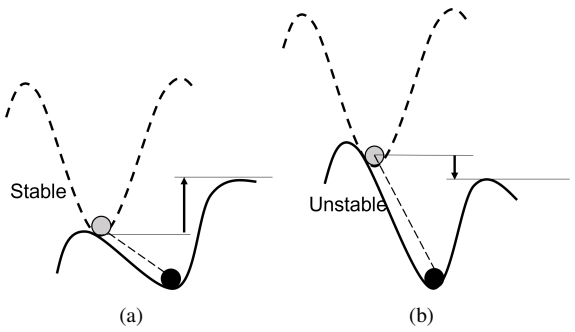

Fig. 1. Illustration of the energy function method (a) stable case, (b) unstable case

therefore the influence of the rotor speeds can be neglected at this situation. The energy of the system mainly relies on the system total potential energy. Details are shown in Section II Part A.

The principle of the energy function on evaluating generation synchronization is illustrated in Fig. 1(a) and (b). The dotted curve represents the pre-disturbance system energy surface, and the grey ball shows the pre-disturbance system equilibrium. The solid curve represents the post-disturbance system energy surface, and the black ball is the-post-disturbance system equilibrium. The equilibrium of the pre-disturbance system is in the basin of the pre-disturbance system energy surface, so does the equilibrium of the post-disturbance system since the minimum potential energy is at the equilibrium [2]. To predict if the pre-disturbance equilibrium is in the basin of attraction of the post-disturbance equilibrium, one need to know if the total potential energy of the pre-disturbance equilibrium is higher than the edge of the post-disturbance system energy surface. Fig. 1(a) shows a stable case where the height of the grey ball relative to the black ball represents its potential energy with respect to the post-disturbance system energy surface. The grey ball is released at a height lower than the edge of the black surface so it can not run out of the basin. Fig. 1(b) shows an unstable case. The grey ball is released at a height higher than the edge of the black edge so it can run out of the basin .

A. Transient Stability Energy Function

The energy function shown in this section is widely applied in power system area [1] but the kinetic energy term is not included in our situation since the transient speed is not introduced in the quasi-steady-state simulation. The energy function includes three terms as shown in (1). The first two terms are called potential energy, where the first term is the total work done by the mechanical torque on each rotor, the second term is the magnetic energy, and the third term is the stored dissipation energy. Actually, these three terms in total can be regarded as system total potential energy.

$$V(\tilde{\boldsymbol{\delta}}) = \sum_{i=1}^{m} P_{mi}^{'}(\tilde{\delta}_i - \tilde{\delta}_i^s) - \sum_{i=1}^{m-1}\sum_{j=i+1}^{m} C_{ij}(\cos\tilde{\delta}_{ij} - \cos\tilde{\delta}_{ij}^s) + \sum_{i=1}^{m-1}\sum_{j=i+1}^{m}\int_{\tilde{\delta}_i^s+\tilde{\delta}_j^s}^{\tilde{\delta}_i+\tilde{\delta}_i} D_{ij}\cos\tilde{\delta}_{ij}\, d(\tilde{\delta}_i - \tilde{\delta}_j) \tag{1}$$

where $\tilde{\delta}_i$ is the rotor angle of the ith generator, $\tilde{\delta}_{ij}$ is the rotor angle difference between the ith and jth generators. $\tilde{\delta}_i^s$ is the stable equilibrium of the ith generator, $\tilde{\delta}_{ij}^s$ is the angle difference between $\tilde{\delta}_i^s$ and $\tilde{\delta}_j^s$. $P_{mi}^{'}$ is the mechanical power acting on the ith rotor. C_{ij} is a constant considering the ith row and the jth column of the Kron-reduced susceptance matrix B and the ith and the jth entries of the generator internal voltage vector E. D_{ij} is another constant considering the ith row and the jth column of the Kron-reduced conductance matrix G and the ith and the jth entries of the generator internal voltage vector E. The expressions of these constants are presented in the following.

$$C_{ij} = C_{ji} = E_i^{'}E_j^{'}B_{ij}, D_{ij} = D_{ji} = E_i^{'}E_j^{'}G_{ij} \tag{2}$$

The integration term in (1) depends on a path in which the grey ball will run to position of the black ball. The path of the grey ball moving towards the position of the black ball need to be considered and it is reasonable to assume that the grey ball can roll toward the position of the black ball along the line connecting the two balls. Therefore the integration term can be evaluated approximately based on (3).

$$\int_{\tilde{\delta}_i^s+\tilde{\delta}_j^s}^{\tilde{\delta}_i+\tilde{\delta}_i} D_{ij}\cos\tilde{\delta}_{ij}\, d(\tilde{\delta}_i - \tilde{\delta}_j) \approx D_{ij}\frac{\tilde{\delta}_i + \tilde{\delta}_j - (\tilde{\delta}_i^s + \tilde{\delta}_j^s)}{\tilde{\delta}_{ij} - \tilde{\delta}_{ij}^s}(\sin\tilde{\delta}_{ij} - \sin\tilde{\delta}_{ij}^s) \tag{3}$$

B. The edge of the post-disturbance system energy surface

In order to identify the edge of the post-disturbance energy surface, a direction in which the grey ball will roll toward the position of the black ball need to be specified. The direction indicates a path. Given the pre-disturbance equilibrium and the post-disturbance equilibrium, it is naturally to consider the direction that is along the line connecting the two equilibrium.

An unit directional vector $\overrightarrow{\boldsymbol{u}}$, along which the grey ball is assumed to roll toward the position of the black ball, is defined.

$$\overrightarrow{\boldsymbol{u}} = \frac{\tilde{\boldsymbol{\delta}} - \tilde{\boldsymbol{\delta}}^s}{||\tilde{\boldsymbol{\delta}} - \tilde{\boldsymbol{\delta}}^s||} \tag{4}$$

where $\tilde{\boldsymbol{\delta}}^s \in \boldsymbol{R}^{n\times 1}$ is the estimation of the post-disturbance system equilibrium. $\tilde{\boldsymbol{\delta}} \in \boldsymbol{R}^{n\times 1}$ is the estimation of the pre-disturbance system equilibrium. $||\cdot||$ is the vector norm operator.

To search for the edge of the energy surface, a depth d is defined to show how far the searching is conducted. The edge of the energy surface can be identified by finding out the

978-1-6654-0823-3/22/$31.00 ©2022 IEEE

point $\boldsymbol{p}_i$ that has a maximum energy $V_{\max}$ along the defined direction $\overrightarrow{\boldsymbol{u}}$ within depth d starting from the post-disturbance equilibrium, $\tilde{\boldsymbol{\delta}}^s$.

$$\boldsymbol{p}_{i+1} = \boldsymbol{p}_i + h\overrightarrow{\boldsymbol{u}} \tag{5}$$

where h is a searching step along the defined direction. $\boldsymbol{p}_0 = \tilde{\boldsymbol{\delta}}$ is the first point whose total potential energy needs to be evaluated. The energy of the post-disturbance equilibrium on the post-disturbance system energy surface is zero. The edge energy as $\max V(\boldsymbol{p}_i)$ can be identified, when $V(\boldsymbol{p}_i) > V(\boldsymbol{p}_{i-1})$ and $V(\boldsymbol{p}_i) > V(\boldsymbol{p}_{i+1})$ and $||\boldsymbol{p}_{\text{end}} - \tilde{\boldsymbol{\delta}}|| < d$. If the energy function is changing monotonously along $\overrightarrow{\boldsymbol{u}}$, then the $\max V(\boldsymbol{p}_i)$ is on the boundary of the searching domain.

Thus one can evaluate if the pre-disturbance equilibrium is in the basin of attraction of the post-disturbance equilibrium by comparing $V(\tilde{\boldsymbol{\delta}})$ and $V(\boldsymbol{p}_i)$. If $V(\tilde{\boldsymbol{\delta}}) > V(\boldsymbol{p}_i)$, then pre-disturbance equilibrium is not in the basin of attraction, if $V(\tilde{\boldsymbol{\delta}}) < V(\boldsymbol{p}_i)$, then the pre-disturbance equilibrium is in the basin of attraction.

C. Discussion

In this paper, a disturbance of line outages is considered, which do not introduce transient kinetic energy of the system, and then an exist point energy can be employed as a threshold. Because the first swing transient stability can be determined by the energy of the exist point. While the energy function need to adopt the energy of a controlled unstable equilibrium [13] as a threshold when a specific fault can introduce transient kinetic energy.

III. Case Study

In this section, the effectiveness and the accuracy of the quasi-dynamic energy function method for out-of-step prediction are test on the IEEE 39-bus 10-machine system under $N-k$ line outages, where k is up to 3. The effectiveness of the energy function are illustrated by considering outages of three lines at the same time under different loading conditions, and then the accuracy of the energy function are evaluated by testing $N-k$ line outages.

To show the effectiveness of the energy function on evaluating synchronization from one equilibrium to another equilibrium, a case study is conducted on IEEE 39-bus 10-machine system. This case study considers outages of three lines at the same time. They are line 1, line 3 and line 20. Two scenarios with two different loading conditions are studied to demonstrate stable case and unstable case, respectively. The first scenario is in a normal loading condition, the second scenario increases the load by 50%. The searching depth d and searching step are 6 and 0.2, respectively. Thus $||\boldsymbol{p}_{\text{end}} - \tilde{\boldsymbol{\delta}}|| < 6$ rad and $\boldsymbol{p}_{\text{end}} = \boldsymbol{p}_{30}$ since $\frac{d}{h} = \frac{6}{0.2} = 30$. The energy function value of 30 intervals for each scenario can be checked.

A stable case is shown in Fig. 2. The energy of the pre-disturbance equilibrium in the normal loading condition is at the height of the grey ball as shown in Fig. 2(a). The edge of the post-disturbance energy surface along the direction $\overrightarrow{\boldsymbol{u}}$ starting from the pre-disturbance equilibrium is at $V(\boldsymbol{p}_{24})$. Since the grey ball's height $V(\boldsymbol{p}_1) = V(\tilde{\boldsymbol{\delta}}) = 0.88$ is less than the edge energy $V(\boldsymbol{p}_{24}) = 1.35$, the grey ball cannot rush out of the basin of the energy surface. The energy function indicates that the pre-disturbance equilibrium is in the basin of attraction of the post-disturbance equilibrium based on the post-disturbance energy surface. The verification is done on this scenarios as shown in Fig. 2(b). A dynamic simulation of the post-disturbance system is conducted, where the dynamics of each generator is modeled as a classical generator model. The initial rotor angles are set to be the pre-disturbance equilibrium, the initial rotor speeds are set to be zeros. The rotor angles experience some transient periods during the first 15 sec and then they are synchronized into the post-disturbance system equilibrium.

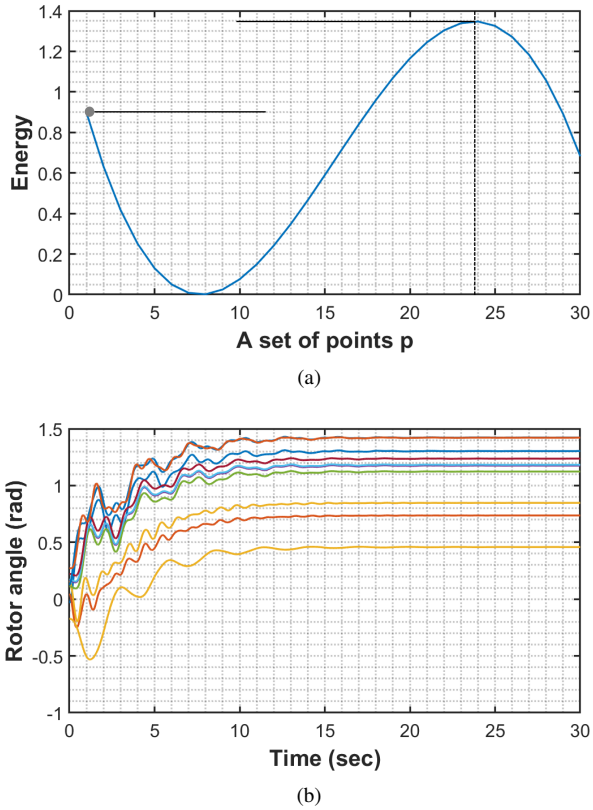

(a)

(b)

Fig. 2. A stable case evaluated via the energy function method (a) energy surface, (b) simulation verification

An unstable case is shown in Fig. 3. The energy of the pre-disturbance equilibrium in the second scenario is at the height of the grey ball in Fig. 3(a). The edge of the post-disturbance energy surface along the direction $\overrightarrow{\boldsymbol{u}}$ starting from the pre-disturbance equilibrium is at $V(\boldsymbol{p}_{13})$. Since the grey ball's height $V(\boldsymbol{p}_1) = V(\tilde{\boldsymbol{\delta}}) = 0.054$ is larger than the edge energy $V(\boldsymbol{p}_{13}) = 0.5 \times 10^{-6}$, the grey ball can rush out of the basin of the energy surface. The energy function indicates that the pre-disturbance equilibrium is out of the basin of attraction of the post-disturbance equilibrium based on the post-disturbance system energy surface. The verification is done on this scenarios as shown in Fig. 3(b). The dynamic

978-1-6654-0823-3/22/$31.00 ©2022 IEEE

simulation setting is the same with the stable case scenarios. The initial rotor angles are set to be the pre-disturbance equilibrium, the initial rotor speeds are set to be zeros. The 10 generators experience some transient periods during the first 5 sec and then they are running into an asynchronous condition into three groups. As shown in Fig. 3(a), the negative energy after the edge of the energy surface, which is the 13th point in our case, is not accurate since the energy function is a local energy evaluated based on the post-disturbance network. So one do not interpret the energy after the edge.

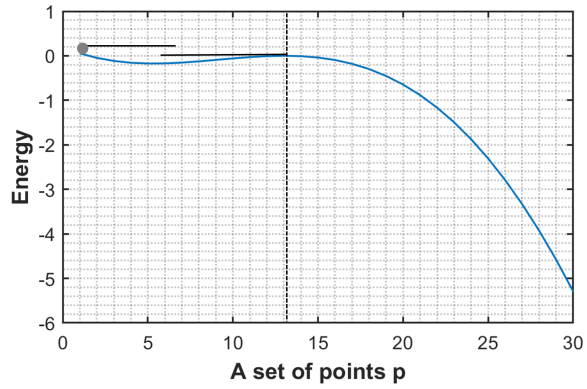

(a)

(b)

Fig. 3. An unstable case evaluated via the energy function method (a) energy surface, (b) simulation verification

To show the accuracy of the energy function on evaluating synchronization subjected to line outages, $N-1$, $N-2$ and $N-3$ tests are conducted on the IEEE 39-bus 10-machine system. There are totally 34 lines in the tested system so there are 34, 561 and 5984 scenarios in the $N-1$, $N-2$ and $N-3$ tests, respectively.

Firstly, the energy function method is tested in the normal loading condition with one-line-outage at a time for each scenario (the $N-1$ test), there are 34 scenarios. There is one scenario that the power flows are not convergent after screening all one-line-outage. The other 33 scenarios are all transient stable as indicated by the energy function method since the edge of the energy surface is much higher than the energy of the pre-disturbance equilibrium in all these scenarios. And these transient stable scenarios are also verified via corresponding dynamic simulations.

In the $N-2$ test, there are $\frac{34\times33}{2}=561$ scenarios in total including 11.41% divergent scenarios and 88.59% convergent scenarios. Among the convergent scenarios (energy function is applicable), there are 4 unstable scenarios and 493 stable scenarios as indicated by the energy function method and all verified by dynamic simulations. 492 stable cases have zero deviation from synchronous speed and 1 stable case has a deviation of 0.18rad/s. This scenario is shown in Fig. 4.

In the $N-3$ test, there are $\frac{34\times33\times32}{3\times2}=5984$ scenarios in total including 25.58% divergent scenarios and 74.42% convergent scenarios. Among the convergent scenarios, there are 118 unstable scenarios and 4335 stable cases as indicated by the energy function method. 112 out of 118, which is 94.92% unstable scenarios, and 4315 out of 4335, which is 99.54% stable scenarios, can be verified by the corresponding dynamic simulations. Fig. 5 shows one unstable scenario but identified as a stable scenario and Fig. 6 shows one stable scenario but identified as an unstable scenario. It is worth to mention that the energy of the pre-disturbance equilibrium is much smaller than zero, means that the pre-disturbance equilibrium can roll away from the post-disturbance equilibrium so the the pre-disturbance equilibrium is out of the basin of attraction of the post-disturbance equilibrium. This scenario can be verified by dynamic simulations and is shown in Fig. 7.

To test the performance of energy function on a heavy loading condition in the power grid, a limit of the grid is found as the nose point on the PV curve. The heavy loading condition represents that the grid operates at 80% of its limit. In the heavy loading condition, there are 11.76%, 31.55%, 59.63% divergent power flow in $N-1$, $N-2$ and $N-3$ tests, respectively. Table I provides the accuracy of the energy function method in different loading conditions. The accuracy is calculated based on the convergent scenarios only since the divergent issue is not the focus of this paper. It is shown that the energy function has 100% accuracy in the $N-1$ and the $N-2$ test, and has a 99.41% accuracy in the $N-3$ test running at a normal loading condition, while has 96.67%, 91.41% and 80.75% accuracy in $N-1$, $N-2$ and $N-3$ tests, respectively in the heavy loading condition.

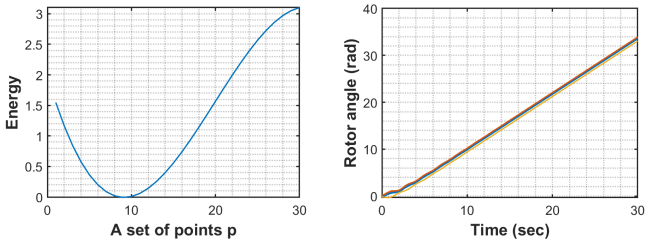

(a)

(b)

Fig. 4. N-2 synchronous case evaluated via the energy function method (a) energy surface, (b) simulation verification

978-1-6654-0823-3/22/$31.00 ©2022 IEEE

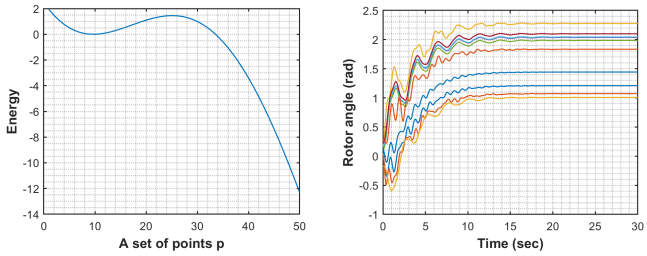

(a) (b)

Fig. 5. N-3 synchronous case wrongly evaluated via the energy function method (a)energy surface (b)simulation verification

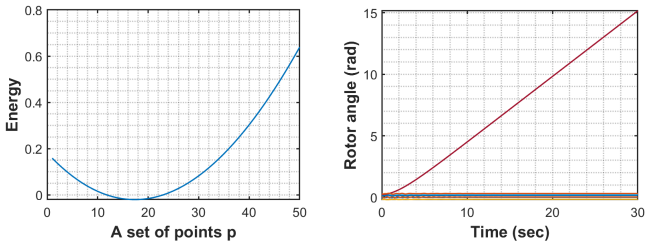

(a) (b)

Fig. 6. N-3 asynchronous case wrongly evaluated via the energy function method (a)energy surface (b)simulation verification

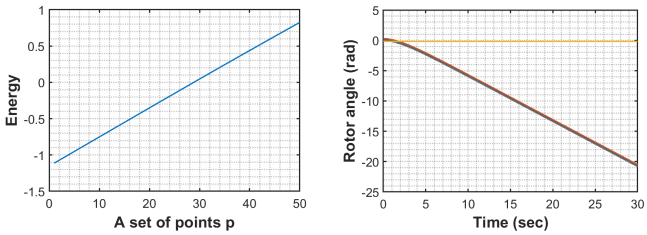

(a) (b)

Fig. 7. N-3 asynchronous case wrongly evaluated via the energy function method (a)energy surface (b)simulation verification

TABLE I
ENERGY FUNCTION ACCURACY TEST RESULTS

Margin	loading	N-1	N-2	N-3
60%	normal	100%	100%	99.41%
20%	heavy	96.67%	91.41%	80.75%

IV. CONCLUSION

This paper proposes an energy function method to evaluate the transient stability of power system subjected to line-outages. This approach can be applied to quasi-dynamics power system simulations without imposing time-consuming dynamic simulations. The energy function is to evaluate whether the pre-disturbance equilibrium is in the basin of attraction of the post-disturbance equilibrium. Test cases are implemented on the IEEE 39-bus 10-machine system. The transient stability evaluated by the energy function method has a 100% accuracy on the $N-1$ and $N-2$ test, and has a 99.41% accuracy on the $N-3$ test in the normal loading condition, while has 96.67%, 91.41% and 80.75% accuracy in $N-1$, $N-2$ and $N-3$ tests, respectively, in the heavy loading condition.

REFERENCES

[1] Sun, K., Likhate, S., Vittal, V., Kolluri, V.S. and Mandal, S., 2007. An online dynamic security assessment scheme using phasor measurements and decision trees. IEEE transactions on power systems, 22(4), pp.1935-1943.

[2] Wehenkel, L., Van Cutsem, T. and Ribbens-Pavella, M., 1989. An artificial intelligence framework for online transient stability assessment of power systems. IEEE Transactions on Power Systems, 4(2), pp.789-800.

[3] Xu, Y., Dong, Z.Y., Zhao, J.H., Zhang, P. and Wong, K.P., 2012. A reliable intelligent system for real-time dynamic security assessment of power systems. IEEE Transactions on Power Systems, 27(3), pp.1253-1263.

[4] He, M., Zhang, J. and Vittal, V., 2013. Robust online dynamic security assessment using adaptive ensemble decision-tree learning. IEEE Transactions on Power systems, 28(4), pp.4089-4098.

[5] Wang, X.F., Song, Y. and Irving, M., 2010. Modern power systems analysis. Springer Science & Business Media.

[6] Pai, M.A., Padiyar, K.R. and Radhakrishna, C., 1981. Transient stability analysis of multi-machine AC/DC power systems via energy-function method. IEEE Transactions on Power Apparatus and Systems, (12), pp.5027-5035.

[7] Michel, A., Fouad, A. and Vittal, V., 1983. Power system transient stability using individual machine energy functions. IEEE Transactions on Circuits and Systems, 30(5), pp.266-276.

[8] Varaiya, P., Wu, F.F. and Chen, R.L., 1985. Direct methods for transient stability analysis of power systems: Recent results. Proceedings of the IEEE, 73(12), pp.1703-1715.

[9] Hiskens, I.A. and Hill, D.J., 1989. Energy functions, transient stability and voltage behaviour in power systems with nonlinear loads. IEEE transactions on power systems, 4(4), pp.1525-1533.

[10] Fouad, A.A. and Vittal, V., 1991. Power system transient stability analysis using the transient energy function method. Pearson Education.

[11] Chiang, H.D., 1989. Study of the existence of energy functions for power systems with losses. IEEE Transactions on Circuits and Systems, 36(11), pp.1423-1429.

[12] Vu, T.L. and Turitsyn, K., 2015. Lyapunov functions family approach to transient stability assessment. IEEE Transactions on Power Systems, 31(2), pp.1269-1277.

[13] Chiang, H.D., Wu, F.F. and Varaiya, P.P., 1994. A BCU method for direct analysis of power system transient stability. IEEE Transactions on power systems, 9(3), pp.1194-1208.

[14] Sun, K., Hou, Y., Sun, W., Qi, J., 2018. Power System Control under Cascading Failures: Understanding, Mitigation and System Restoration, Wiley-IEEE Press. ISBN: 978-1-119-28202-0.

[15] Sun, K., 2018. WAMS Based Controlled System Separation to Mitigate Cascading Failures in Smart Grid, Smart Grid Control: Opportunities and Research Challenges, Springer. ISBN: 978-3-319-98310-3.

[16] Ding, L., Guo, Y., Wall, P., Sun, K., 2018. Vladimir Terzija, Identifying the Timing of Controlled Islanding Using a Controlling UEP based Method, IEEE Transactions on Power Systems, 33(6), pp.5913-5922.

[17] Sun, K., Hur, K., Zhang, P., 2011. A New Unified Scheme for Controlled Power System Separation Using Synchronized Phasor Measurements, IEEE Transactions on Power Systems, 26(3), pp.1544-1554.

[18] Ju, W., Sun, K., Yao, R., 2019. Interaction Graph-Based Active Islanding to Mitigate Cascading Outages, IEEE PES General Meeting in Atlanta, GA.

[19] Mei, S., He, F., Zhang, X., Wu, S. and Wang, G., 2009. An improved OPA model and blackout risk assessment. IEEE Transactions on Power Systems, 24(2), pp.814-823.

[20] Ju, W., Sun, K. and Yao, R., 2018. Simulation of cascading outages using a power-flow model considering frequency. IEEE Access, 6, pp.37784-37795.

[21] Chen, C., Ju, W., Sun, K. and Ma, S., 2019. Mitigation of cascading outages using a dynamic interaction graph-based optimal power flow model. IEEE Access, 7, pp.168637-168648.

978-1-6654-0823-3/22/$31.00 ©2022 IEEE